SCIENCE CHINA
Information Sciences

• MOOP •

March 2026, Vol. 69, Iss. 3, 134301:1–134301:3
https://doi.org/10.1007/s11432-025-4704-9

Real-time integrated 2.04 cm range resolution and 16.14-Gbps bidirectional wireless communication in photonic-assisted millimeter wave band system over 100 m

Qihang WANG, Wen ZHOU*, Jie ZHANG, Jingtao GE, Sicong XU, Siqi WANG, Xin LU, Jiali CHEN, Chengzhen BIAN, Xiongwei YANG, Weiping LI, Kaihui WANG & Jianjun YU*

Key Laboratory for Information Science of Electromagnetic Waves (MoE), and State Key Laboratory of ASIC and System, School of Information Science and Technology, Fudan University, Shanghai 200433, China

Received 6 May 2025/Revised 30 September 2025/Accepted 3 December 2025/Published online 20 January 2026

Citation Wang Q H, Zhou W, Zhang J, et al. Real-time integrated 2.04 cm range resolution and 16.14-Gbps bidirectional wireless communication in photonic-assisted millimeter wave band system over 100 m. Sci China Inf Sci, 2026, 69(3): 134301, https://doi.org/10.1007/s11432-025-4704-9

Millimeter wave integration of sensing and communication (MMW-ISAC) is a promising technology. By extending the spectrum, the ISAC system can achieve potentially higher communication rates and sensing accuracy. To overcome the bandwidth limitations of radio frequency electronic devices, researchers have proposed photonic-assisted up-conversion schemes to generate MMW waves to achieve ultra-wideband sensing and communication [1]. Photonic-assisted MMW-ISAC systems offer significant advantages such as expanded bandwidth, license-free operation, and enhanced security [2, 3]. According to the latest research, thanks to the ultra-large bandwidth, the photonic-assisted MMW-ISAC system can simultaneously achieve centimeter-level resolution and a data rate up to tens of Gbit/s [4–7]. However, these results have short wireless transmission distances (<20 m), and the digital signal processing (DSP) is implemented offline (OL). In addition, they are currently still in the primary stage, and the transmission modes are mainly unidirectional. In autonomous driving, intelligent transportation, UAV cooperation (both cross-domain and air-to-ground), as well as satellite and industrial park monitoring tasks, the simultaneous availability of communication and sensing capabilities at long ranges is indispensable for timeliness, safety, and practicality. For example, in autonomous driving on highways, an ISAC system must provide coverage of at least several hundred meters to leave sufficient time for risk detection, reaction, and execution of avoidance maneuvers. Importantly, all these scenarios involve multi-node systems (e.g., vehicle fleets, UAV swarms, satellite constellations), where one-way sensing alone is insufficient for collaborative positioning or joint perception. In contrast, bidirectional (BiDi) ISAC enables distributed sensing and communication, allowing multiple nodes to exchange measurements. For instance, in UAV formation flying and cross-domain cooperation, bi-directional ranging supports centimeter- to decimeter-level relative positioning while maintaining a low-latency communication link, thereby ensuring formation stability and coordinated task execution. Therefore, BiDi ISAC over long ranges is not merely a technical enhancement, but a prerequisite for the reliable deployment of next-generation intelligent transportation and autonomous systems. In this work, we demonstrate a BiDi photonic-assisted MMW real-time ISAC experimental system. The system uses the waveform of discrete multi-tone (DMT) and implements real-time DSP based on the FPGA hardware platform. The system can achieve a data rate of 16.14 Gbps and a range resolution of 2.04 cm over 100 m wireless distance. Figure 1(a) shows the experimental setup of our proposed real-time BiDi photonic-assisted MMW-ISAC system. For the base station (BS) and user equipment (UE), the real-time transceiver is implemented at one FPGA platform: Xilinx AUV901 FPGA, equipped with a 6-bit 29.4912 GSa/s DAC and ADC. Sensing is achieved through the two-way time-of-flight (TW-ToF) principle, which uses the flight time of the ISAC signal between the two asynchronous transceivers of the BS and UE to estimate the range.

The signal flight time is calculated based on the time when the UE sends the signal (t_1), the time when the BS receives the signal sent by the UE (t_2), the time when the BS returns the signal (t_3), and the time when the UE receives the BS return signal (t_4). Among them, the exact arrival time of the signal (t_4 and t_2) is estimated by the FPGA master clock difference and the ADC sampling signal synchronization timestamp. After subtracting the system fixed wired link delay (t_0), the estimated range is expressed as $R_{\text{Esti.}} = \frac{(t_4-t_1)-(t_3-t_2)-t_0}{2} \times c$, where $(t_4 - t_1)$ is equal to the master clock difference between the UE signal transmission and reception added with the local signal synchronization timestamp, $(t_3 - t_2)$ is equal to the system fixed processing time of the BS minus the synchronization timestamp of the BS, t_0 is the system wired link delay calibrated by the reference experiment with the true range (R_{True}) equal to 0, and c is the speed of light. This scheme effectively eliminates the error introduced by the device clock mismatch, ensuring high accuracy of the range estimation. Considering that the synchronization timing accuracy is 1/29.4912 GHz = 0.0339 ns, the theoretical range resolution of this scheme can be calculated as $\Delta R_{\text{Esti.}} = \frac{0.0339}{2} \times c = 0.508$ cm. At the UE transmitter side, the real-time DMT-ISAC signal is

* Corresponding author (email: zwen@fudan.edu.cn, jianjun@fudan.edu.cn)

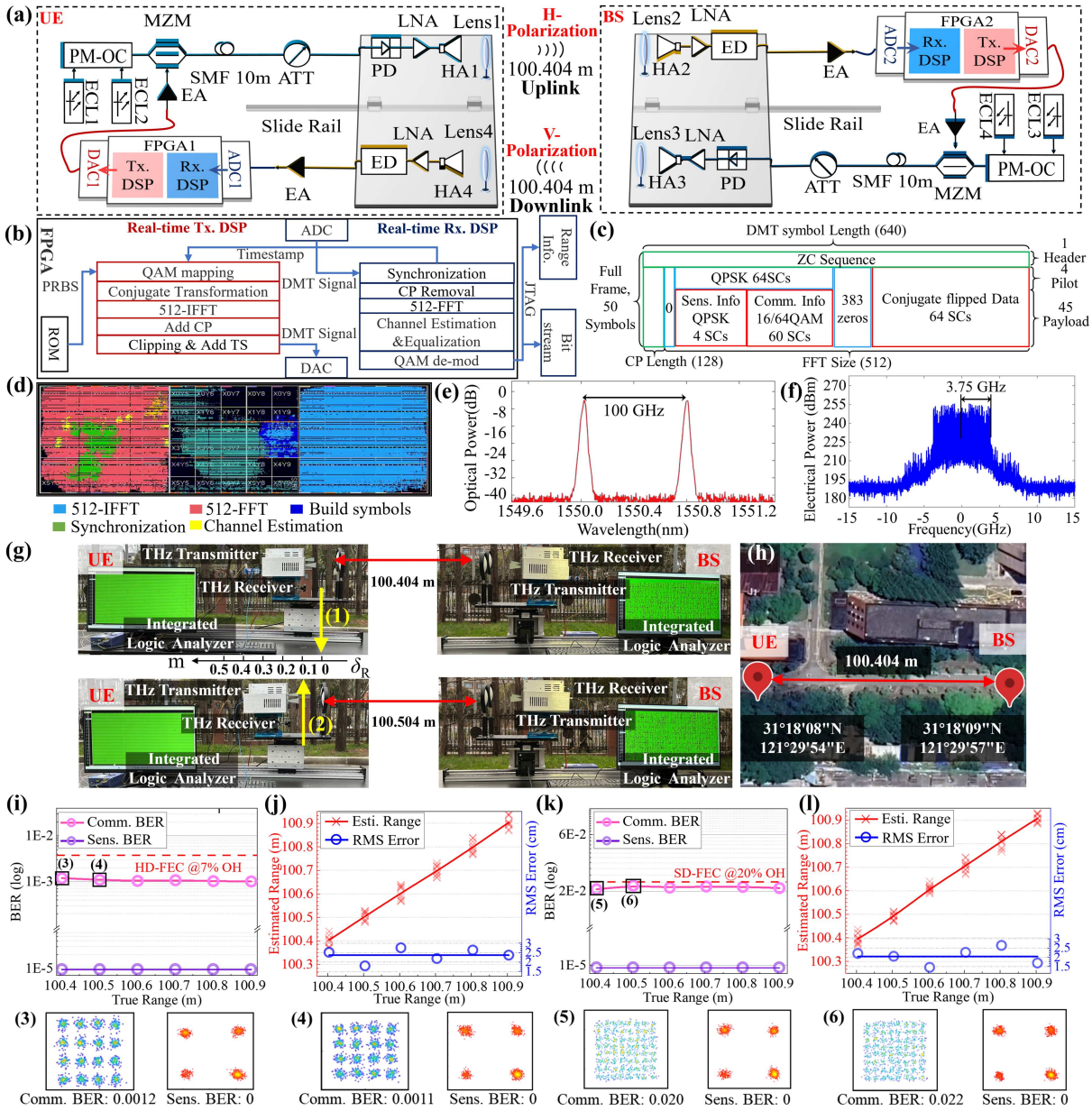

Figure 1 (Color online) Experimental setup of the real-time BiDi photonic-assisted MMW ISAC system. (a) System diagram. (b) Real-time DSP flow based on the FPGA. (c) DMT signal structure. (d) Resource utilization of the FPGA. (e) Optical spectrum measured after PM-OC. (f) 64QAM- DMT-ISAC electrical spectrum. (g) Experimental scene of (1) $\delta R = 0$ m and (2) $\delta R = 0.1$ m. (h) Satellite image of the experimental system. (i) BER results, (3) and (4) constellation diagrams and (j) sensing results of the 16QAM-DMT-ISAC signal. (k) BER results, (5) and (6) constellation diagrams and (l) sensing results of the 64QAM-DMT-ISAC signal.

generated by the transmitter DSP process shown in Figure 1(b). The PRBS is generated and stored in the read-only memory of the FPGA, combined with the local 8-bit synchronization timestamp as ISAC information, and is fed into the QAM mapping module. The sensing information is mapped to QPSK considering the robustness under low signal-to-noise ratio (SNR) conditions, and the communication information is mapped to 16-/64-QAM with adjustable rates. Subsequently, the QAM symbols are conjugated and arranged to be Hermitian symmetric.

The 512 complex-valued QAM symbols are sent to a 512-point IFFT module (128-path in parallel) to obtain 512-length real-valued data. A 128-length cyclic prefix is added to the data to resist inter-symbol interference (ISI), resulting in a complete 640-length DMT payload symbol, as shown in Figure 1(c). The DMT signals are then digitally clipped to reduce the PAPR and DAC quantization noise, scaled to 6 bits to match the DAC resolution.

At last, one 640-length Zadoff-Chu (ZC) sequence as a synchronization symbol and four offline-generated QPSK-DMT symbols as pilot symbols are sequentially added before the 45 payload symbols to form a complete ISAC frame. Figure 1(d) shows the resource utilization of the FPGA platform.

The real-time generated signals drive the Mach-Zehnder modulator (MZM) through a 15 dB electric amplifier (EA). Two free-running laser diodes (ECL1 and ECL2) with a frequency interval of 100 GHz are coupled by a polarization-maintaining optical coupler (PM-OC). The optical spectrum after PM-OC is shown in Figure 1(e). After 10 m standard single-mode fiber (SSMF) transmission, a single-ended photodiode (PD, Finisar XPDV4120R) is

employed to convert the optical signal into a 100 GHz signal via optical heterodyne beating.

The generated MMW signal is amplified by a low-noise amplifier (LNA) operating at 75–110 GHz with a gain of 35 dB and sent to free space through a horn antenna (HA1) with a gain of 25 dBi. A pair of lens antennas with a total gain of 30 dB is used to realize 100 m BiDi communication. After wireless transmission, the DMT-ISAC signal is captured by HA2 and amplified by a 35 dB LNA. The signal is fed to an envelope detector (ED, 3 GHz 3 dB bandwidth, 75–110 GHz detector) for frequency down-conversion in the BS receiver. Figure 1(f) shows the received 64QAM-ISAC-DMT electrical spectrum, where the signal bandwidth is 3.75 GHz.

The baseband signal is amplified by a 25 dB EA and sampled by the ADC. The 6-bit sampled signals are fed into the FPGA to perform real-time receiver DSP. After symbol synchronization and CP removal, a 512-point FFT (128-path in parallel) is performed to obtain the frequency-domain DMT signal. Subsequently, a zero-forcing channel estimation (CE) module is used to estimate the channel response and compensate for the received signals. Finally, the compensated QAM symbols are demapped to recover the bitstream. The downlink is similar to the uplink described above except for the antenna's polarization direction, mainly to reduce the crosstalk with the uplink. The maximum achievable range of this system is estimated to be 0.65 km. Detailed calculations are provided in Appendix B.

In the field experiment, we controlled the slide rail at UE via a stepper motor with a positioning accuracy of 0.1 mm to displace δR = 0–0.5 m in incremental steps of 0.1 m, as shown in Figure 1(g). We established the initial ground-truth range R_0 = 100.404 m using an RTK survey instrument at δR = 0, as shown in Figure 1(h).

For the 16QAM-DMT-ISAC signal, the bit error rate (BER) of communication 16-QAM and sensing QPSK signals are shown in Figure 1(i). The 16-QAM achieves a BER under the 7% hard-decision FEC threshold, corresponding to a data rate: 3.75 Gbaud $\times \frac{60}{64} \times 4$ bit/symbol $\times \frac{45}{49} \Big/ (1 + 7\%) = 12.07$ Gbit/s. The BER of the QPSK remains below 1×10^{-5} at each position, ensuring sensing reliability. Insets (3) and (4) show the symbol constellations when R_{True} = 100.404 m and 100.504 m, respectively.

The sensing results are shown in Figure 1(j). For the result shown in Inset (3) of Figure 1, $R_{\text{True}} = R_0 + \delta R = 100.404 + 0 =$ 100.404 m. Here $t_3 - t_2$ = 649.1089 ns, $t_4 - t_1$ = 1499.6677 ns, and t_0 = 180.8336 ns. The estimated range is calculated as $R_{\text{Esti.}} = \frac{(t_4 - t_1) - (t_3 - t_2) - t_0}{2} \times c = 100.389$ m. The error to R_{True} is 0.015 m, and the root mean squared error (RMSE) of 10 measurements is 2.51 cm. Moreover, the 16QAM-DMT-ISAC signal achieves an average RMSE of 2.37 cm across all test positions.

For the 64QAM-DMT-ISAC signal, the BER results of 64-QAM and sensing QPSK are shown in Figure 1(k). Insets (5) and (6) show the symbol constellations when R_{True} = 100.404 m and 100.504 m, respectively. The 64-QAM signals maintain a BER below the 20% soft-decision threshold at all positions, corresponding to a peak data rate of 16.14 Gbit/s. The sensing results are shown in Figure 1(l), and the average RMSE is 2.04 cm across all test positions. The error in range estimation is mainly caused by the clock deviation ($\sim$0.03 ns) due to crystal oscillator instability.

We demonstrate a real-time MMW 100 m ISAC system with 16.14 Gbps data rate and 2.04 cm range resolution. To our knowledge, this is the first real-time demonstration of a BiDi photonic-assisted MMW-ISAC system.

Acknowledgements This work was partially supported by National Key R&D Program of China (Grant No. 2023YFB2905600), National Natural Science Foundation of China (Grant Nos. 62127802, 62331004, 62305067, U24B20142, U24B20168, 62427815), and Key Project of Jiangsu Province of China (Grant No. BE2023001-4).

Supporting information Appendixes A and B. The supporting information is available online at info.scichina.com and link.springer.com. The supporting materials are published as submitted, without typesetting or editing. The responsibility for scientific accuracy and content remains entirely with the authors.

References

1 Kittlaus E A, Eliyahu D, Ganji S, et al. A low-noise photonic heterodyne synthesizer and its application to millimeter-wave radar. Nat Commun, 2021, 12: 4397
2 Mallick K, Mandal P, Dutta B, et al. Bidirectional OFDM based MMW/THzW over fiber system for next generation communication. IEEE Photonics J, 2021, 13: 1–7
3 Mallick K, Mandal P, Mukherjee R, et al. Generation of 40 GHz/80 GHz OFDM based MMW source and the OFDM-FSO transport system based on special fine tracking technology. Optical Fiber Tech, 2020, 54: 102130
4 Lei M, Zhu M, Cai Y, et al. Integration of sensing and communication in a W-band fiber-wireless link enabled by electromagnetic polarization multiplexing. J Lightwave Technol, 2023, 41: 7128–7138
5 Liu J, Yu J, Zhao X, et al. W-band photonics-aided ISAC wireless system sharing OFDM signal as communication and sensing. In: Proceedings of Optical Fiber Communication Conference and Exhibition, 2024
6 Li L, Zhang L, Zhang H, et al. THz-over-fiber system with orthogonal chirp division multiplexing for integrated sensing and communication. J Lightwave Technol, 2024, 42: 176–183
7 Lyu Z, Zhang L, Zhang H, et al. Multi-channel photonic THz-ISAC system based on integrated LFM-QAM waveform. J Lightwave Technol, 2024, 42: 3981–3988